

Contents lists available at [ScienceDirect](http://www.sciencedirect.com)

Biochimica et Biophysica Acta

journal homepage: www.elsevier.com/locate/bbamem

On-line identification of P-glycoprotein substrates by monitoring of extracellular acidification and respiration rates in living cells

Swen Seeland^{a,c}, Alexander Treiber^a, Mathias Hafner^{b,c}, Jörg Huwyler^{d,*}^a Actelion Pharmaceuticals Ltd., Gewerbestrasse 16, 4123 Allschwil, Switzerland^b Institute for Molecular and Cell Biology, University of Applied Science, Paul-Wittsack Strasse 10, 68163 Mannheim, Germany^c Medical Faculty Mannheim, University of Heidelberg, Theodor-Kutzer-Ufer 1-3, 68167 Mannheim, Germany^d Division of Pharmaceutical Technology, Department of Pharmaceutical Sciences, University of Basel, Klingelbergstrasse 50, 4056 Basel, Switzerland

ARTICLE INFO

Article history:

Received 23 December 2010

Received in revised form 10 March 2011

Accepted 11 March 2011

Available online 22 March 2011

Keywords:

P-glycoprotein

ABCB1

Drug transport

Multi-drug resistance

Microsensor

ABSTRACT

The influence of P-glycoprotein (ABCB1) in drug resistance as well as drug absorption and disposition is an important factor to be considered during the development of new drugs. Thus, the early identification and exclusion of compounds showing a high affinity towards P-glycoprotein can help to select drug candidates. The aim of our study was to implement a label-free assay for the identification of P-glycoprotein substrates in living cells. For this approach, a multiparametric, chip-based sensor system was used to determine extracellular acidification, cell respiration and adhesion upon stimulation with P-glycoprotein substrates. Using L-MDR1 cells, a human P-glycoprotein overexpressing cell line, the influence of P-glycoprotein activity was determined for seven different compounds, demonstrating the applicability of the system for P-glycoprotein substrate identification. Effects were concentration dependent, as shown for the P-glycoprotein substrate verapamil, and were associated with cellular acidification and respiration. P-glycoprotein ATPase activation by verapamil could be described by a Michaelis–Menten type kinetic profile showing saturation at high substrate concentrations. The Michaelis–Menten constants K_M were determined to be 0.92 μM (calculated based on extracellular acidification) and 4.9 μM (calculated based on cellular respiration). Control experiments using 100 nM of the P-glycoprotein inhibitor elacridar indicated that the observed effects were related to P-glycoprotein ATPase activity. In contrast, wild-type LLC-PK1 cells not expressing P-glycoprotein were not responsive towards stimulation with different P-glycoprotein substrates. Summarizing these findings, the used microsensor system is a generic system suitable for the identification of P-glycoprotein substrates. In contrast to biochemical P-glycoprotein assays, activation of the drug efflux pump can be monitored on-line in living cells to identify P-glycoprotein substrates and to study the molecular mechanisms of adenosinetriphosphate-dependent active transport.

© 2011 Elsevier B.V. All rights reserved.

1. Introduction

ATP-binding cassette (ABC) transporters are one of the largest families of multidomain integral membrane proteins that use the energy of ATP hydrolysis to translocate molecules across cellular membranes. They are found in all species including man [1]. These efflux pumps recognize a wide range of chemically diverse endogenous and exogenous compounds and act as gatekeepers contributing in cellular defense [2,3]. They are involved in biomedical phenomena like multidrug-resistance of cancer cells or poor bioavailability

of drugs [4]. One of the best characterized ABC transporters is P-glycoprotein (P-gp), the gene product of the human multi-drug resistance (MDR1) gene and the first member of subfamily B of the ABC transporters (ABCB1). P-gp is highly expressed in human tissues with protective function and is found on the luminal surface of cellular barriers including the kidney proximal tubule, small intestine and colon, testis, adrenal cortex and the blood–brain barrier [5]. The expression pattern of P-gp suggests a protective function of P-gp towards potentially toxic xenobiotics. P-gp is a 170 kDa protein consisting of two homologous drug binding transmembrane domains [6] and a cytosolic nucleotide-binding domain with ATPase activity [7]. P-gp has broad substrate specificity and significantly modulates the pharmacokinetics of many chemically unrelated drugs [8]. As a consequence, efficient screening methods are needed to identify substrates or inhibitors of P-gp during the drug discovery and development process [9]. For the identification of P-gp inhibitors, high-throughput fluorescent assays exist such as the rhodamine123 [10] or the calcein-AM [11] assay. However, identification of substrates of P-gp remains a challenge:

Abbreviations: MDR1, multi-drug resistance gene 1 or ABCB1; P-gp, P-glycoprotein; ATP, adenosinetriphosphate; ECAR, extracellular acidification rate; OCR, oxygen consumption rate; SEM, standard error of the mean; IDES, interdigitated electrode structure; ISFET, ion-sensitive field effect transistor

* Corresponding author. Tel.: +41 61 267 15 13; fax: +41 61 267 15 16.

E-mail address: joerg.huwyler@unibas.ch (J. Huwyler).

predictive cellular assays such as the transcellular transport assay [12] or any *in vivo* experimentation relies on sensitive, compound-specific and expensive analytical procedures such as the use of radiolabeled test compounds or quantitative mass spectroscopy. In contrast, generic biochemical assays such as the ATPase release assay [13] make use of membrane preparations of P-gp. However, these assays are not necessarily representative for the *in vivo* situation since membrane integrity is disturbed and the orientation of P-gp binding sites towards the intracellular or extracellular space is lost during the preparation of cell homogenates. It should be noted that for living cells, a label-free and real-time method was introduced recently, which is based on single cell monitoring of drug-related fluorescence [14].

In view of these limitations, the aim of our study was to implement a new label-free method to identify P-gp substrates on-line in living cells and to validate this assay as a generic tool for the reliable identification of P-gp substrates. Regeneration of the consumed ATP via glycolysis is coupled to the formation of carbon dioxide and lactate which are released into the extracellular milieu as carbonic acid and lactic acid [15]. Besides acidification, oxygen is consumed during glycolysis resulting in a decrease of oxygen concentration in the extracellular environment. These two processes, i.e. oxygen consumption and extracellular acidification, are indicators for ATP regeneration, and thus, P-gp activity. Using a microsensor system, a label-free and real-time analyzing system for the identification of P-gp substrates in living cells was established.

2. Materials and methods

2.1. Compounds

Colchicine was from Biochrom AG (Berlin, Germany) and elacridar was obtained from LGM Pharma (Boca Raton, Florida, USA). All other chemicals were purchased from Sigma (Buchs, Switzerland). Ten millimolar stock solutions were prepared using DMSO. The DMSO concentrations in the final solutions did not exceed 0.1% (v/v).

2.2. Cell culture

The human P-gp overexpressing cell line L-MDR1 derived from the porcine kidney epithelial cell line LLC-PK1 was obtained under license from professor Alfred Schinkel, The Netherlands Cancer Institute (Amsterdam, The Netherlands). Cells were maintained under standard cell culture conditions as described previously [8,9]. In brief, cells were cultivated at passage numbers 12–26 in 75 cm² cell culture flasks at 37 °C in medium 199 with GlutaMAX (Gibco/Invitrogen, Basel, Switzerland) supplemented with 50 IU/mL penicillin, 50 µg/mL streptomycin and 10% (v/v) fetal bovine serum (PAA Laboratories, Pasching, Austria) in a humidified atmosphere containing 5% CO₂.

L-MDR1 cells were subcultured in the presence of 150 ng/mL colchicine to maintain P-gp expression levels. Colchicine was omitted from medium 12 h prior to use in the experiments to avoid the development of other drug resistance mechanisms that could modify the action of P-gp [16]. Once in culture and induced, cells have been shown to express constant levels of P-gp for up to 15 passages [17].

2.3. Microsensor experiments

Cells were detached by trypsinization (Invitrogen) and analyzed by a Vi-cell XR cell viability analyzer (Beckman Coulter, Krefeld, Germany). Cells were then diluted in culture medium to reach a final concentration of 2.9×10^5 cells per milliliter medium and a 0.35 mL aliquot of this cell suspension was transferred to a pre-warmed metabolic chip and incubated for at least 16 h prior to use. A Bionas® 1500 microsensor system (Bionas, Rostock, Germany) was used to continuously record cellular physiological parameters. The system was used as described previously [18]. The core of the system

consists of a silicon sensor chip SC1000 (Fig. 1) containing ISFET and Clark-type sensors for the measurement of dynamic changes of acidification and oxygen consumption.

Cell adhesion is monitored by means of impedance measurements using an IDES electronic circuit. The height of the reaction chamber above the sensor surface is 200 µm. Cells were seeded directly onto the silicon chip without prior surface treatment or coating to ensure optimal signal detection. During the experiment, assay medium (see below) was delivered to the cells at a constant flow rate of 250 µL/min. The supply of assay medium was interrupted periodically. This stop/go cycles (Fig. 2) were carried out during the whole experiment. Typically, the stop and pump phases lasted 2 min each. During these “stop phases,” metabolic breakdown products of the cells (lactate and carbonate) were released into the assay medium and were allowed to accumulate resulting in a change of extracellular pH [15]. Extracellular oxygen concentrations were monitored in parallel. Enhanced metabolic activity of cells requires increased oxygen consumption for regeneration of energy, which is detectable during the stop phases by a decrease of the oxygen concentration. Initial rates of extracellular acidification and respiration were calculated by changes of the slope in the stop phases and a linear regression analysis. Rates were standardized to 100% of baseline signal just before compound treatment. Impedance measurements were carried out continuously to monitor cell adhesion, and thus, cell viability and confluence [19]. As a control, 0.2% Triton X-100 was added to the cells at the end of each experiment to induce cell membrane destruction, and thus, detachment of cells from the surface of the sensor chip. By this control, at the end of the experiment, a reference signal of the cell-free sensor surface was obtained (0% control value) [19]. It should be noted that pH values and oxygen concentrations are determined with respect to corresponding reference values. These relative signals are related to a 0% control value of an empty sensor chip and to a 100% reference value representing the baseline signal of a cell coated chip prior to compound treatment.

2.4. System initialization

Prior to each experiment, the supply lines of the system were conditioned in a three-step procedure: disinfection with 70% (v/v) aqueous ethanol, flushing with an excess of phosphate-buffered saline (PBS) and rinsing with low buffered assay medium. For the measurements, an assay medium with low buffer capacity was required. The assay medium was prepared from a 10× concentrated



Fig. 1. Photographic representation of the Bionas chip-based sensor system. The silicon sensor chip has a surface area of 74 mm². Integrated sensors include one IDES for the measurement of cellular impedance, five ISFET sensors for the measurement of pH and five Clark-type oxygen sensors (picture reproduced with permission of Bionas Ltd.).

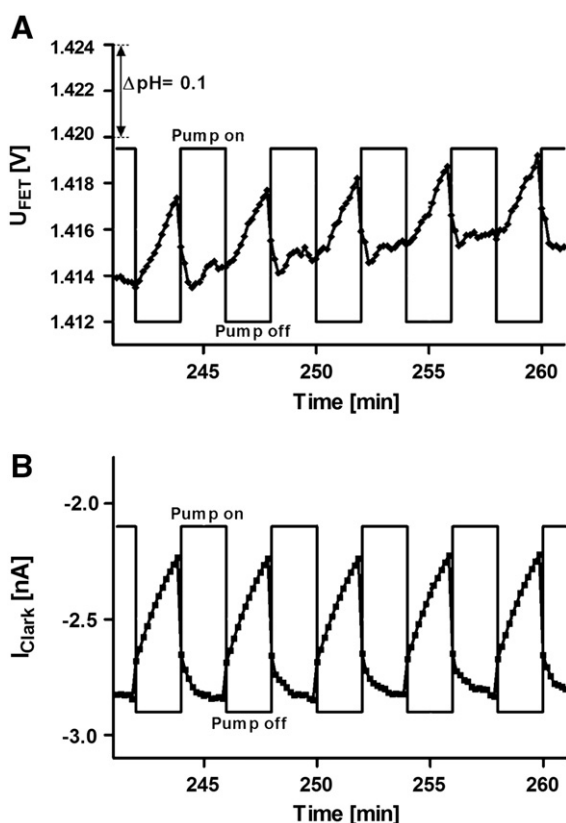


Fig. 2. Representative example of a microsensor experiment. Cellular respiration of L-MDR1 cells is shown during several 2 min stop (pump off) and 2 min go (pump on) cycles (solid lines). Recorded data (square symbols) are plotted against time and include measurement of extracellular acidification (A) and oxygen concentration (B). The pH is proportional to a measured voltage (U) and the oxygen concentration is proportional to a measured current (I). Extracellular acidification (A) and cellular respiration (B) rates were calculated from the initial slope of each stop phase by a linear regression.

medium 199 (Gibco/Invitrogen) supplemented with 0.32 mM Gluta-MAX, 2% (v/v) fetal bovine serum, 50 IU/mL penicillin and 50 μ g/mL streptomycin. The assay medium did not contain $NaHCO_3$. To preserve the osmotic balance of the buffer system, a final concentration of 26.2 mM NaCl was used. The medium was adjusted to pH 7.4. Before use, the integrity of the cell-monolayer covering the surface of the microsensor chip was verified using a Motic DM-39C reflected-light microscope (Motic Group Ltd., Hong Kong, China). Cell monolayers with a cellular confluence below 80% were rejected for use.

2.5. Measurement

Signals from the microsensor chip were recorded after a stabilization phase of at least 4 h. The duration of the stabilization phase was variable and was dependent on the baseline metabolic activity of the cells. Experiments were initiated as soon as a constant baseline signal to noise ratio from the different sensors could be acquired. During 5 go cycles, cells were exposed to different test substances in concentration ranges between 0.1 and 10 μ M dissolved in assay medium.

Raw data were recorded by all sensors in intervals of 10 s to obtain 12 raw data points per stop and go cycle (Fig. 2). From these data points, initial rates of acidification and cellular respiration were derived by linear regression. Stimulation phases with test substances were followed by a wash-out phase of at least 2 h before a new stimulation phase was initiated. These extended wash-out cycles were required to allow for a regeneration of the cells and a complete wash-out of the test substances. After the experiment, impedance

values were recorded following solubilization of cells by 0.2% (v/v) Triton X-100. This control is used to compare cell monolayer integrity during the experiment with a reference value obtained from a cell-free sensor chip at the end of the experiment. This value represents by definition the 0% reference control value (see above).

2.6. Statistics

A two-tailed Mann–Whitney *U* test was used to compare metabolic rate points before and during compound treatment. The level of statistical significance was defined as $p < 0.05$. The statistical calculation of the Mann–Whitney *U* test was performed using GraphPad Prism software (Version 5.03, GraphPad Software Inc., La Jolla, CA, USA). Each experiment was performed at least in triplicates. Results are expressed as the mean \pm SEM, where SEM is the standard error of the mean.

3. Results and discussion

In the present study, a multiparametric, chip-based sensor system (Fig. 1) was used for real-time identification of P-glycoprotein (P-gp) substrates in human P-gp overexpressing LLC-PK1 cells (L-MDR1). The used microsensor system is an analytical tool for on-line monitoring of changes in extracellular acidification rate (ECAR), cell respiration (oxygen consumption rate—OCR) and cell adhesion (Fig. 2). The results obtained with P-gp overexpressing L-MDR1 cells were compared with those of wild-type LLC-PK1 cells exhibiting only a marginal P-gp expression [20]. Seven marketed drugs, known to be substrates or non-substrates of P-gp, were used as reference compounds for system validation: caffeine and propranolol are not substrates of P-gp whereas verapamil, daunorubicin, fexofenadine, quinidine and loperamide are known substrates of the transporter. In contrast to previous studies in which pH microsensors were used for mechanistic studies on P-gp ATPase activation [21], our experiments included measurements of cellular oxygen consumption and cell adhesion and were focused on efficient identification of P-gp substrates.

The microsensor assay was optimized with respect to maximal stimulation amplitudes to allow for a sensitive and reliable recording of signals. Important assay parameters included the use of an assay medium with a low buffer capacity supplemented with 2% (w/v) fetal bovine serum albumin. Serum proteins reduce unspecific binding of test compounds to surfaces such as the plastic tubings of the microsensor instrument and enhance cellular viability in the assay system during incubation times of up to 24 h. Optimal cell densities were in a range of 0.75 to 1.5×10^4 attached cells per chip. The design of the actual incubation chamber (i.e. the volume of the 200 μ m space between the surface of the sensor chip and the chamber lid) is of critical importance. In our experimental set-up, the effective volume of the incubation chamber was 5.6 μ L. Such a minimal volume is needed to monitor the rate of accumulation of metabolic products and depletion of oxygen in the assay medium. A further reduction of the incubation chamber volume led to system instability and a high signal-to-noise ratio of the measured signal. During measurements, the flow of assay medium was periodically interrupted for 2 min. After each measuring period, the incubation chamber was flushed for another 2 min with assay medium before a new measuring cycle was initiated. Prolonged phases of reduced flow of assay medium should be avoided due to detrimental effects on cell viability and overall system stability. Viability of cells was monitored continuously by measurements of cellular impedance. Deviations in the range of less than $\pm 15\%$ from initial values over a run time of 1500 min were considered to be acceptable and were attributed to cell proliferation or small morphological changes after compound treatment, i.e. shrinking or swelling. Experiments were discontinued as soon as a change in impedance in excess of these limits was recorded.

In a first set of experiments, activity of P-gp was monitored in the presence of verapamil (a P-gp substrate [9,22]) and the negative control caffeine [23]. Experiments were initiated as soon as a stable baseline metabolic rate was attained (100% threshold in Fig. 3). ECAR as well as OCR could be identified to correlate with P-gp activation (Fig. 3, phase 1 of the experiment). Selectivity of the observed P-gp stimulatory effects were demonstrated by inhibition of P-gp activity with elacridar (GF120918), a selective third-generation P-gp inhibitor [24,25] (Fig. 3, phase 3). Elacridar on its own does not stimulate P-gp ATPase activity but has a slight inhibitory effect on overall metabolic activity of L-MDR1 cells (Fig. 3, phase 2). At the end of the experiment (Fig. 3, phase 4), reference 0% signal-levels of the microsensor chip were determined by Triton X-100-mediated removal of attached cells.

Observed acidification rates and respiration rates increased in the presence of increasing concentrations of up to 15 μM verapamil (Fig. 4, black symbols) and followed Michaelis–Menten type kinetics. Stimulation of P-gp by verapamil showed saturation at high concentrations and was characterized by a K_M value of $0.92 \pm 0.12 \mu\text{M}$ (calculated based on ECAR, mean \pm SEM, $n=4$) and $4.9 \pm 2.7 \mu\text{M}$ (calculated based on OCR, mean \pm SEM, $n=4$). These values are in good agreement with a K_M value of $1.5 \mu\text{M}$ reported previously [26] for the stimulation of P-gp by verapamil at low substrate concentrations. It is important to note that for the first time (to our knowledge) P-gp activation was monitored not only by extracellular acidification [26] but also by stimulation of cellular respiration. In our experimental setup, ECAR deliver stronger and more reliable signals as compared to OCR: V_{max} values for ECAR ($57.4 \pm 1.6\%$ as compared to 0% control, mean \pm SEM, $n=4$) were twice as high as the corresponding V_{max} values for OCR ($25.4 \pm 5.2\%$ as compared to 0% control, mean \pm SEM, $n=4$). At substrate concentrations of 50 μM verapamil, a sudden drop in ECAR as well as in OCR was observed and could be attributed to either cellular toxicity or substrate inhibition at high concentrations [21] of the test compound (Fig. 4). However, for none of the tested verapamil concentrations, cell impedance deviated from 100% control values by more than $\pm 13\%$. In a separate set of control experiments (Fig. 4, open symbols), P-gp-deficient LLC-PK1 cells were incubated in the presence of verapamil and did not show any stimulation effects in either ECAR or OCR. Again, high concentrations of verapamil (50 μM) seemed to inhibit cellular metabolic activity.

The question arises, whether ECAR or OCR should be used to monitor P-gp activation. Both parameters can be used to monitor cellular responses upon stimulation of cells using P-gp substrates and are therefore correlated. ECAR is predominantly linked to glycolysis

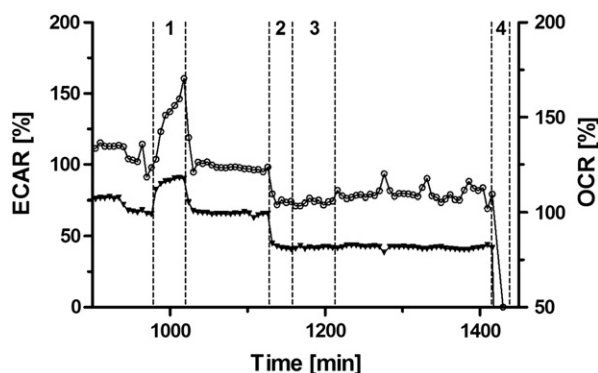


Fig. 3. Stimulation of P-gp overexpressing L-MDR1 cells in the presence and absence of the P-gp inhibitor elacridar. Phase 1: stimulation of L-MDR1 cells with 10 μM verapamil results in extracellular acidification (ECAR, \circ) and increased oxygen consumption rate (OCR, \blacktriangledown). Phase 2: addition of 100 nM elacridar after a wash-out phase. Phase 3: addition of 10 μM verapamil in the presence of 100 nM elacridar. Phase 4: Triton X-100 (0.2%, v/v) treatment at the end of the experiment to obtain the 0% reference value of the empty sensor chip.

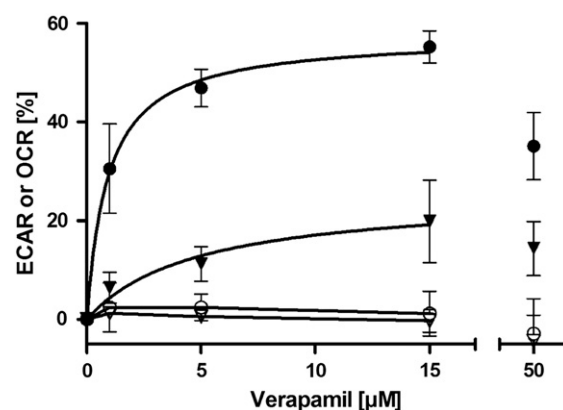


Fig. 4. Stimulation of P-gp in the presence of different concentrations of verapamil. Extracellular acidification (ECAR, circles) and oxygen consumption (OCR, triangles) in P-gp overexpressing L-MDR1 cells (solid symbols) and wild-type LLC-PK1 (open symbols) cells measured as a function of increasing concentrations of verapamil. Solid lines: curve fitting using a Michaelis–Menten type kinetics model. Signals obtained at verapamil concentration of 50 μM were rejected for kinetic calculations. Level of significance between L-MDR1 and LLC-PK1 controls: $p < 0.001$, $n=4$.

whereas OCR is indicative of mitochondrial respiration. In our experiments (Figs. 3 and 4), extracellular acidification was demonstrated to deliver a three-fold higher signal than oxygen consumption. In addition, baseline respiration rates changed over time during prolonged experimental periods. It is tempting to speculate that overall cellular viability and/or possibly mitochondrial toxicity might be confounding factors influencing cellular respiration in an unpredictable way. In view of the reduced sensitivity as well as the uncertainty associated with the OCR parameter, it was decided to quantitate P-gp stimulation based on extracellular acidification only, but to monitor OCR values as an additional control in parallel to identify cell-permeating compounds affecting mitochondrial respiration.

The chip-based sensor system was also used to identify substrates of P-gp. Representative examples of marketed drugs are shown in Fig. 5. Activation of P-gp was expressed as ratio between acidification rates measured during and immediately before stimulation of L-MDR1 cells (ΔECAR). Propranolol, caffeine, quinidine, verapamil and loperamide were used at a substrate concentration of 10 μM . The

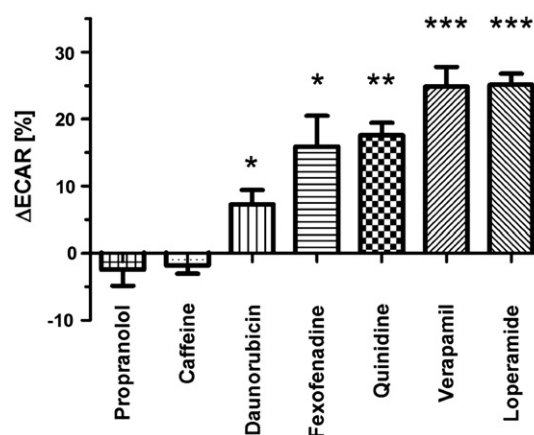


Fig. 5. Identification of P-gp substrates using the microsensor system in combination with P-gp overexpressing L-MDR1 cells. Extracellular acidification rates were determined in the presence and absence of test compound (10 μM final substrate concentration with the exception of 1 μM of daunorubicin and fexofenadine). Ratios between acidification rates before and during stimulation (ΔECAR) are shown. Data are means \pm SEM, $n > 3$. Levels of statistical significant difference between acidification rates in unstimulated or stimulated cells are $p < 0.05$ (*), $p = 0.01$ (**) or $p < 0.001$ (***).

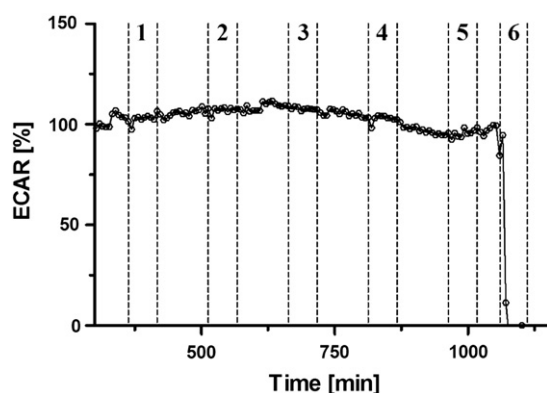


Fig. 6. Control experiments demonstrating absence of stimulatory effects in wild type LLC-PK1 cells. Caffeine (phase 1), verapamil (phase 2), loperamide (phase 3), quinidine (phase 4) and paclitaxel (phase 5) did not induce extracellular acidification (ECAR) in P-gp deficient LLC-PK1 cells. All compounds were tested at a substrate concentration of 10 μ M. Triton X-100 (0.2%, v/v) treatment (phase 6) at the end of the experiment was used to obtain the 0% reference value of the cell-free sensor chip.

substrate concentrations of daunorubicin and fexofenadine had to be reduced to 1 μ M to avoid cellular toxicity. Propranolol and caffeine, which do not interact with P-gp, were used as negative controls. All P-gp substrates were correctly identified and showed statistically significant differences ($p < 0.05$) in ECAR as compared to the negative controls. Cellular impedance, and thus, cellular viability were not affected by the test compounds in the used concentration range. Absence of cellular toxicity or unspecific stimulatory effects was confirmed in a set of control experiments (Fig. 6). None of our test compounds stimulated ECAR using the P-gp-deficient LLC-PK1 cell line under the same experimental conditions.

4. Conclusions

In the present study, stimulation of P-gp was monitored by the measurement of extracellular acidification. In addition, cellular respiration was used for the first time as an indicator of P-gp-related metabolic activity. The microsensor assay was demonstrated to be a sensitive, label-free and generic method to identify substrates of P-gp and to determine kinetic parameters of P-gp ATPase activation such as the Michaelis–Menten constant, K_M . One sensor chip can be used for multiple consecutive measurements. A critical factor for such measurements is the intrinsic toxicity of test compounds, which may lead to cellular stress, and hence, unspecific metabolic activation of the target cell as soon as a critical substrate concentration threshold is reached. It is therefore necessary to test different substrate concentrations in P-gp-deficient LLC-PK1 control cells prior to the actual experiment in L-MDR1 cells. In the present study (as demonstrated in Fig. 6), substrate concentrations of test compounds (e.g., 1 or 10 μ M) were chosen in accordance with these principles to avoid artifacts and toxic effects. The need for time-consuming control experiments limits the throughput of the microsensor system. A solution to this problem might be the use of a multiple-sensor system, in which several test compounds can be measured in parallel in a semi-automated and cost-efficient way. Such systems may offer additional advantages in that ABC transporters other than P-gp might be investigated based on their ATPase activity.

Conflict of interest statement

The authors have no conflicts of interest to disclose.

Acknowledgments

We thank Dr. Jérôme Segrestaa (Actelion Pharmaceuticals Ltd.) for his continuous support. The excellent technical support of Andreas Flüeli is acknowledged.

References

- [1] P.M. Jones, A.M. George, The ABC transporter structure and mechanism: perspectives on recent research, *Cell. Mol. Life Sci.* 61 (2004) 682–699.
- [2] M.M. Gottesman, S.V. Ambudkar, Overview: ABC transporters and human disease, *J. Bioenerg. Biomembr.* 33 (2001) 453–458.
- [3] T. Litman, T.E. Druley, W.D. Stein, S.E. Bates, From MDR to MXR: new understanding of multidrug resistance systems, their properties and clinical significance, *Cell. Mol. Life Sci.* 58 (2001) 931–959.
- [4] M.I. Borges-Walmsley, K.S. McKeegan, A.R. Walmsley, Structure and function of efflux pumps that confer resistance to drugs, *Biochem. J.* 376 (2003) 313–338.
- [5] F. Thiebaut, T. Tsuruo, H. Hamada, M.M. Gottesman, I. Pastan, M.C. Willingham, Cellular localization of the multidrug-resistance gene product P-glycoprotein in normal human tissues, *Proc. Natl. Acad. Sci. U.S.A.* 84 (1987) 7735–7738.
- [6] Y. Raviv, H.B. Pollard, E.P. Bruggemann, I. Pastan, M.M. Gottesman, Photosensitized labeling of a functional multidrug transporter in living drug-resistant tumor cells, *J. Biol. Chem.* 265 (1990) 3975–3980.
- [7] I.L. Urbatsch, B. Sankaran, S. Bhagat, A.E. Senior, Both P-glycoprotein nucleotide-binding sites are catalytically active, *J. Biol. Chem.* 270 (1995) 26956–26961.
- [8] A.H. Schinkel, E. Wagenaar, L. van Deemter, C.A. Mol, P. Borst, Absence of the mdr1a P-Glycoprotein in mice affects tissue distribution and pharmacokinetics of dexamethasone, digoxin, and cyclosporin A, *J. Clin. Invest.* 96 (1995) 1698–1705.
- [9] D. Schwab, H. Fischer, A. Tabatabaei, S. Poli, J. Huwyler, Comparison of in vitro P-glycoprotein screening assays: recommendations for their use in drug discovery, *J. Med. Chem.* 46 (2003) 1716–1725.
- [10] G.D. Eytan, R. Regev, G. Oren, C.D. Hurwitz, Y.G. Assaraf, Efficiency of P-glycoprotein-mediated exclusion of rhodamine dyes from multidrug-resistant cells is determined by their passive transmembrane movement rate, *Eur. J. Biochem.* 248 (1997) 104–112.
- [11] F. Tiberghien, F. Loo, Ranking of P-glycoprotein substrates and inhibitors by a calcein-AM fluorometry screening assay, *Anticancer Drugs* 7 (1996) 568–578.
- [12] A. Braun, S. Hammerle, K. Suda, B. Rothen-Rutishauser, M. Gunthert, S.D. Kramer, H. Wunderli-Allenspach, Cell cultures as tools in biopharmacy, *Eur. J. Pharm. Sci.* 11 (Suppl 2) (2000) S51–S60.
- [13] B. Sarkadi, E.M. Price, R.C. Boucher, U.A. Germann, G.A. Scarborough, Expression of the human multidrug resistance cDNA in insect cells generates a high activity drug-stimulated membrane ATPase, *J. Biol. Chem.* 267 (1992) 4854–4858.
- [14] X. Li, V. Ling, P.C. Li, Same-single-cell analysis for the study of drug efflux modulation of multidrug resistant cells using a microfluidic chip, *Anal. Chem.* 80 (2008) 4095–4102.
- [15] E. Thedinga, A. Kob, H. Holst, A. Keuer, S. Drechsler, R. Niendorf, W. Baumann, I. Freund, M. Lehmann, R. Ehret, Online monitoring of cell metabolism for studying pharmacodynamic effects, *Toxicol. Appl. Pharmacol.* 220 (2007) 33–44.
- [16] M.M. Hoffman, L.Y. Wei, P.D. Roepe, Are altered pH and membrane potential in hu MDR 1 transfectants sufficient to cause MDR protein-mediated multidrug resistance? *J. Gen. Physiol.* 108 (1996) 295–313.
- [17] J.W. Polli, S.A. Wring, J.E. Humphreys, L. Huang, J.B. Morgan, L.O. Webster, C.S. Serabjit-Singh, Rational use of in vitro P-glycoprotein assays in drug discovery, *J. Pharmacol. Exp. Ther.* 299 (2001) 620–628.
- [18] E. Thedinga, A. Ullrich, S. Drechsler, R. Niendorf, A. Kob, D. Runge, A. Keuer, I. Freund, M. Lehmann, R. Ehret, In vitro system for the prediction of hepatotoxic effects in primary hepatocytes, *ALTEX* 24 (2007) 22–34.
- [19] R. Ehret, W. Baumann, M. Brischwein, A. Schwinde, B. Wolf, On-line control of cellular adhesion with impedance measurements using interdigitated electrode structures, *Med. Biol. Eng. Comput.* 36 (1998) 365–370.
- [20] K. Takara, M. Tsujimoto, M. Kokufu, N. Ohnishi, T. Yokoyama, Up-regulation of MDR1 function and expression by cisplatin in LLC-PK1 cells, *Biol. Pharm. Bull.* 26 (2003) 205–209.
- [21] E. Gatlik-Landwojtowicz, P. Aanismaa, A. Seelig, Quantification and characterization of P-glycoprotein–substrate interactions, *Biochemistry* 45 (2006) 3020–3032.
- [22] E.C. Spoelstra, H.V. Westerhoff, H.M. Pinedo, H. Dekker, J. Lankelma, The multidrug-resistance-reverser verapamil interferes with cellular P-glycoprotein-mediated pumping of daunorubicin as a non-competing substrate, *Eur. J. Biochem.* 221 (1994) 363–373.
- [23] L. Smetanova, V. Stetinova, D. Kholova, J. Kvetina, J. Smetana, Z. Svoboda, Caco-2 cells and Biopharmaceutics Classification System (BCS) for prediction of transepithelial transport of xenobiotics (model drug: caffeine), *Neuro Endocrinol. Lett.* 30 (Suppl 1) (2009) 101–105.
- [24] F. Hyafil, C. Vergely, P. Du Vignaud, T. Grand-Perret, In vitro and in vivo reversal of multidrug resistance by GF120918, an acridonecarboxamide derivative, *Cancer Res.* 53 (1993) 4595–4602.
- [25] C. Martin, G. Berridge, P. Mistry, C. Higgins, P. Charlton, R. Callaghan, The molecular interaction of the high affinity reversal agent XR9576 with P-glycoprotein, *Br. J. Pharmacol.* 128 (1999) 403–411.
- [26] E. Landwojtowicz, P. Nervi, A. Seelig, Real-time monitoring of P-glycoprotein activation in living cells, *Biochemistry* 41 (2002) 8050–8057.